LONG LIFE FATIGUE PROPERTIES OF FERRITE-PEARLITIC DUCTILE CAST IRON WITH SHOT-PEENING TREATMENT

Yasuo OCHI, Takeshi SEKINO and Takashi MATSUMURA

Department of Mechanical Engineering and Intelligent Systems,
University of Electro- Communications, Tokyo
1-5-1, Chofugaoka, Chofu, Tokyo 182-8585, JAPAN

ABSTRACT

Rotating bending fatigue tests were carried out on specimens of ferrite-pearlitic ductile cast irons (FPDI) with a shot-peening (SP) treatment. Influences of the SP treatment on the fatigue property was investigated experimentally, and the change of an initial residual stress induced by the SP treatment was discussed. As results, the fatigue strength was improved markedly by the SP treatment, but the S-N diagram showed a two-step bending behavior in long life region over 10^7 cycles. The surface hardened layer and the compressive residual stresses were observed more than 300μm from the surface. Sites of the fatigue crack initiation were transferred from the surface to subsurface in the range of longer life region over 7×10^6 cycles region. The initial compressive residual stress was released partially by higher level stress cycling, however, it was almost constant during the lower level stress cycling.

INTRODUCTION

Ductile cast irons (DI) have recently been noticed as one of the renewal materials because of their enough strength, ductility and toughness being equal to steels as good as their easiness of manufacturing. Therefore, the DI materials have various uses for automobile parts and other manufacturing parts for purposes of the reduction of weight and the economical reason [1]. The DI materials have a number of graphites and casting defects as stress concentrators in fatigue crack initiation sites. Then, many researches about the effects of those defects on the fatigue properties have been carried out until now [2~6]. On the other hand, it is well known that a shot-peeing (SP) treatment is one of the effective method for the improvement of fatigue strength [7,8], and it is useful practically for the automobile parts. However, it has not been investigated sufficiently effects of the SP treatment on the fatigue property such as a fracture mechanism and characteristics of S-N diagram in the short and the long life region of the DI materials.

In this paper, rotating bending fatigue tests were carried out on specimens of ferrite-pearlitic ductile cast irons (FPDI) with the SP treatment, and effects of the SP treatment on fracture morphologies and fatigue properties were investigated. It is expected that the SP treatment results not only the high level of work-hardening and the high compressive residual stress, but also, the decrease in casting defects in near surface layer, and then, they lead a considerable improvement of fatigue strength. Therefore, the initial distributions of hardness and the residual stress in the surface hardened layer by the SP treatment were measured, then, the changes in the initial residual stress

were discussed during cyclic stressing. Furthermore, differences in fatigue fracture morphologies in the short and the long regions of fatigue life were discussed from detailed observations of crack initiation sites with a scanning electron microscopy.

EXPERIMENTAL PROCEDURE

The material used in this study was a ferrite-pearlitic ductile cast iron (FPDI), and the chemical compositions (wt.%) are C:3.79, Si:2.20, Mn:0.22, P:0.012, S:0.007 and Mg:0.26, respectively. Surface microstructure is shown in Figure 1 and the structure is composed with distributed spheroidal graphites surrounded by ferrite structure and pearlite structure as a matrix. The characteristics of the microstructure were measured by means of an image processing analysis technique, and the nodularity h_g: 83.7%, the nodule count n_g:175(1/mm^2), the ferritic area fraction f_f:65.1%, the pearlitic area fraction f_p:23.6%, the graphite area fraction f_g:11.3%.

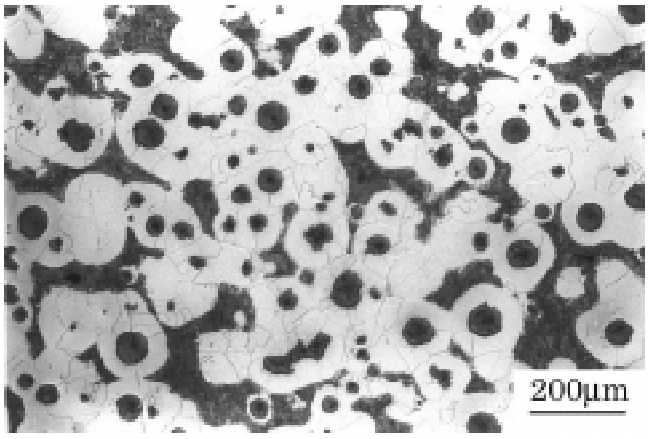

Figure 1 Surface microstructure of FPDI material.

Test specimen is solid round bar type with a shallow groove in the central part as shown in Figure 2. The surface of the specimen was finished with buffing to mirror finish, and this condition of the specimen is named as the AC (as cast) material. The conditions of the shot-peening treatment is as follows; a shot size:ϕ0.6mm steel with a hardness of HCR 53, air pressure: 0.245MPa, and arc height: 0.4mm. The specimens are named as the SP materials. The mechanical properties of both of the AC and the SP materials are almost similar. And the AN (annealed) materials were prepared for reducing the effect of the residual stress, and the annealed condition was 500°C for 2 hrs.

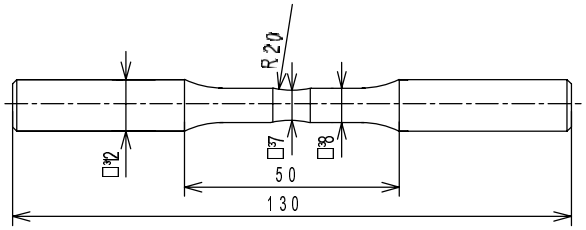

Figure 2 Shape and dimensions of specimen.

The distributions of hardness and residual stress in the internal direction were measured in order to investigate the effects of the SP treatment. Micro-Vickers hardness tester was used for the measurement of hardness distribution of the disc section cut from the SP treated specimens, and the hardness of ferritic area was measured. X-ray diffraction device was used for the measurement of residual stress of specimens surface which was removed repeatedly by electro-polishing. The conditions of X-ray method with Cr-Kα for residual stress measurement is as follows; a diffraction: α-Fe[211], a tube voltage: 30Kv and a tube current: 40mA. Fatigue tests were carried out on the AC, the SP and the AN materials under rotating bending stressing in air at room temperature. The

change of the residual stress during fatigue process was examined by the above X-ray diffraction method. And also, the crack initiation sites were observed for the fracture surface by a electron microscopy (SEM).

EXPERIMENTAL RESULTS AND DISCUSSION

Figure 3 shows the distribution of Vickers hardness in the internal direction from the surface. The hardness distribution of the AC material showed almost constant values, and the surface hardened layer of the SP material was observed more than 300μm depth from the surface. In the AN material, the surface hardened layer was disappeared and the hardness distribution showed almost constant, but the hardness value was lower slightly than the AC material. Figure 4 shows the distribution of the residual stress in the internal direction from the surface. In the AC material, the residual stress showed about zero except the work-hardened layer of very surface by specimen working. In the SP material, the compressive residual stress existed in 500μm depth from the surface, and also, the maximum value of the SP materials was about -450MPa at 20μm depth from the surface. As the surface roughness induced by the SP treatment is assumed to be a factor reducing the fatigue strength, the surface roughness of the SP specimen was measured. The values of the maximum surface roughness R_{max} were 2.8μm, 43.8μm and 43.0μm for the AC, the SP and the AN materials, respectively, and it is clear that the roughness of the SP and the AN material increased remarkably with comparing of that of the AC material.

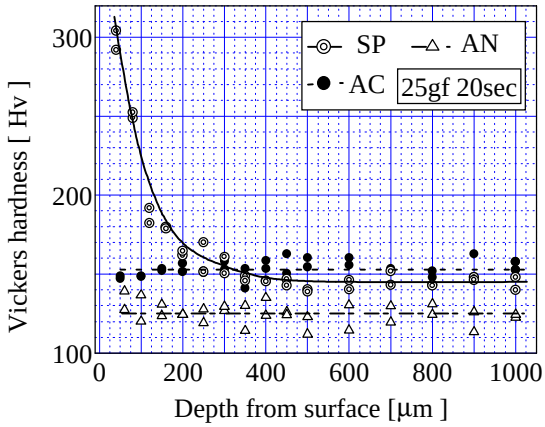

Figure 3 Hardness distribution in the internal direction of the AC, the SP and the AN materials.

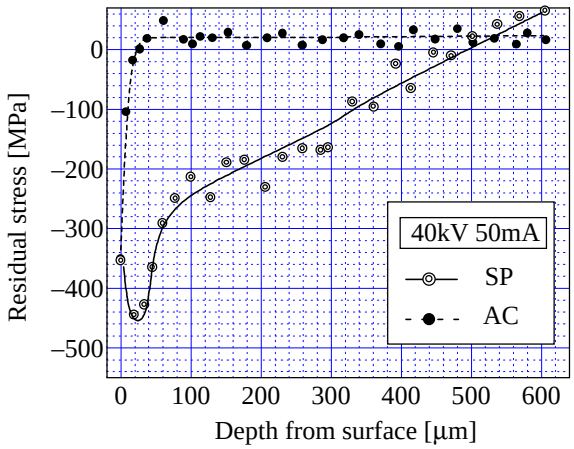

Figure 4 Residual stress distribution in the internal direction of the AC and the SP materials.

Figure 5 shows a typical cross sectional microstructure of the surface hardened layer of the SP material. From the observation, the deformation of the basic matrix of ferrite- pearlitic structure and

the spheroidal graphites occurred by the SP treatment in the region of about 100μm depth from the surface, and the microshrinkages near the surface were not observed because of the SP treatment.

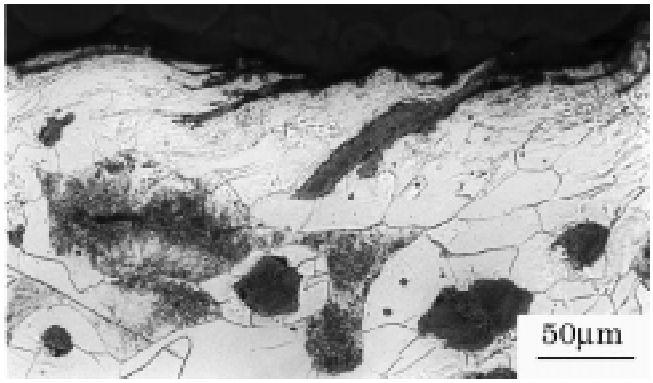

Figure 5 Cross sectional microstructure of the SP material.

Figure 6 shows the results of fatigue tests of the SP, the AC and the AN materials. The fatigue strength of the SP material was improved remarkably comparing with the AC materials, but, the S-N diagram of the SP material showed a two-step bending behavior in the long life region which the apparent horizontal limit existed at the stress amplitude of 350MPa over 10^6 cycles region, and after that the fatigue strength fell down over 10^7 cycles region. This behavior has not been reported about the SP treated DI materials, but there have been reported some times in very long life fatigue region of high strength steels. And, the fatigue limit of the AC material was 220MPa, and then, the fatigue strength of the AN materials showed lower than that of the AC material, and this meant that the fatigue strength was reduced from the notch effects of surface roughness induced by the SP treatment. Both of the S-N diagram of the AC and the AN materials didn't show the two-step bending behavior as like in the case of the SP material.

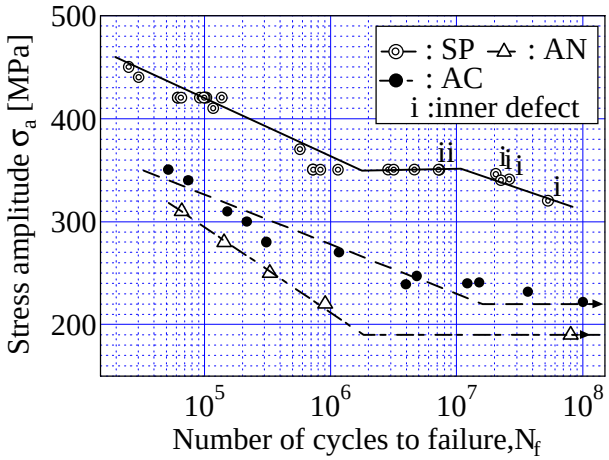

Figure 6 S-N diagrams of the AC, the SP and the AC materials.

From the observations of fracture surfaces of the AC and the SP materials, all the crack initiation sites of the AC materials in whole region of fatigue life, and of the SP materials in the shorter life region before 5×10^6 cycles were gathering graphites or casting defects existing just under the surface as similar as having been reported in the several kinds of DI materials [2~6]. Figure 7 shows an example of the crack initiation site of the SP material. In this case, the stress amplitude σ_a was 370MPa, and the number of cycles to failure N_f was 5.744×10^5 cycles. However, the sites of the fatigue crack initiations of the SP materials in the longer life region than 7×10^6 cycles were transferred from the surface to subsurface, and the crack initiation sites of that case were casting defects existing in over 300μm depth from the surface. Fig.8 shows an example of the fracture surface of the crack initiation site in case of σ_a=346MPa, $N_f=2.05\times10^7$ cycles. In the Figure 6, the

marks i show the specimens fractured from the inner defects. And, the average depth of crack initiation sites existed about 300~700μm and the depth didn't depend on the stress amplitude. And, the root area of the defect size was about 85~195μm, and also didn't depend on the stress amplitude.

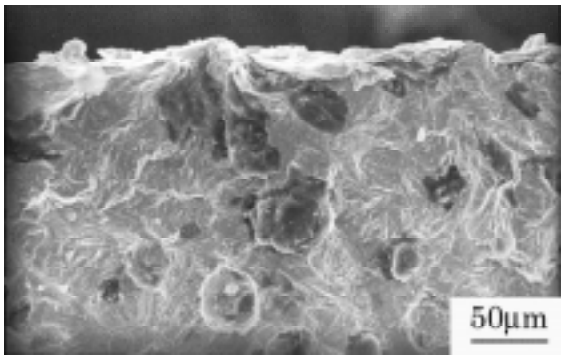

Figure 7 Crack initiation site in the shorter range of fatigue life,
σ_a=370MPa, N_f=5.744×10^5 of the SP material.

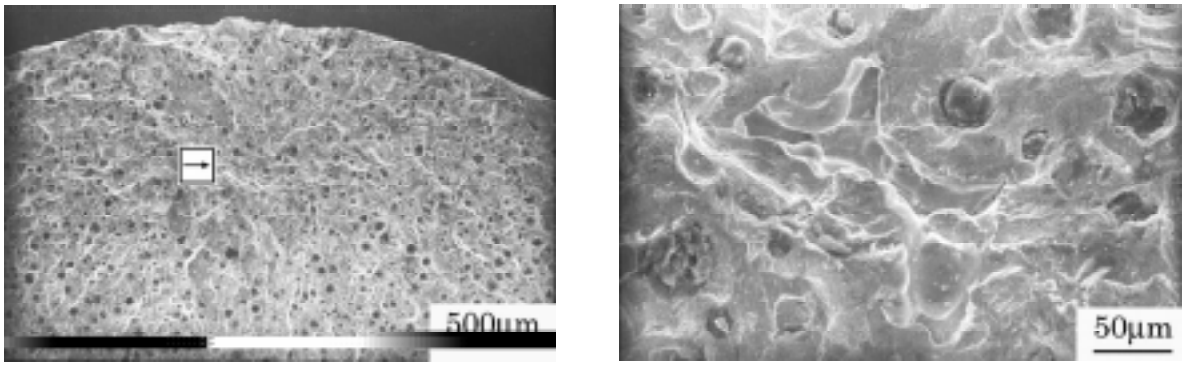

(a) the lower magnification (b) the higher magnification

Figure 8 Crack initiation site in the longer range of fatigue life,
σ_a=346MPa, N_f=2.05×10^7 of the SP material.

Figure 9 shows changes of the compressive residual stresses during fatigue process. The measurement of the residual stress changes were carried out for two levels of stress amplitude; the higher level was 450MPa, being the surface fracture type, and the lower level as 340MPa, being the internal fracture type. From the results, the compressive residual stress in the higher level stress, decreased at very early stage and saturated at the initial cyclic stressing. On the other hand, it was almost constant during fatigue process in the lower level stress cycling.

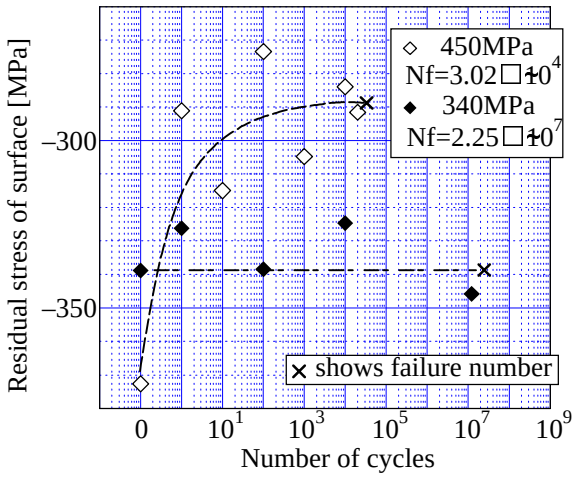

Figure 9 Changes of the surface residual stresses during fatigue process of the SP materials.

From the results of Figure 9, the changes of the initial compressive residual stresses was 80MPa for

σ_a=450MPa, and 0 for σ_a=340MPa, respectively. It has been generally reported that the initial compressive residual stress σ_r decreased when the sum of the σ_r and the loading stress σ_a became larger than the yield stress σ_s [9]. Saruki et al has reported [10] that the residual stress after cyclic loading $|\sigma_{r\ after}|$ could be evaluated from the following Eqn.,

$$|\sigma_{r\ after}| = |\sigma_r| - (|\sigma|_{max} - \sigma_s) \quad (1)$$

where, σ_s in Eqn. (1) is assumed as a relation of σ_s=0.23Hv×9.8. TABLE 1 shows the evaluated value of $|\sigma_{r\ after}|$ from using Eqn. (1). Comparing the values in the TABLE 1 with the experimental values, the both values were almost similar.

TABLE 1 Estimated surface residual stresses after cyclic stressing [MPa].

σ_a	$\|\sigma\|_{max}$	$\|\sigma\|_{max}-\sigma_s$	$\|\sigma_{r\ after}\|$
450	800	100	250
400	750	50	300
350	700	0	350
300	650	0	350

$\sigma_{r\ after}$: Estimated surface residual stress after fatigue test.

CONCLUSION

High cycle fatigue properties in long life region of the SP treated FPDI material was investigated the effects of the SP treatment on the fatigue strength, the fracture morphology and the initial residual stress change induced by the SP treatment. The results obtained in this study are as follows:

1. The fatigue strength at 10^7 cycles of the SP material were improved remarkably comparing with that of the AC material, but the S-N diagram of the SP material showed the two-step bending behavior in the long life region.
2. The fracture sites of the SP materials showed two-type fracture morphology, one was the surface fracture type from the surface defects in the shorter life region before in 5×10^6 cycles, the other was the internal fracture type from the inner defects in the longer life region over in 7×10^6 cycles.
3. The decrease in the initial compressive residual stress depended on the cyclic stress level, in the case of the high level stress amplitude 450MPa, the decrease in the residual stress was 80MPa. The decrease amount was evaluated from the relations of the initial residual stress, the stress amplitude and the yield strength.

References

1. Harada,S., and Kobayashi, T. (1999) Evaluation of Strength of Ductile Cast Irons, AGUNE Technical Center Press.
2. Doi,S., Harada,S., Mitsunaga,K.,Yano.M. and Yasuda,H. (1992), Trans. JSME(A), 58-550, 971.
3. Fukuyama,K., Hasegawa,N. and Nishikawa,Y. (1994) Trans. JSME(A), 60-576,1734.
4. Ochi,Y., Ishii,A., Sasaki,S. and Konishi,Y. (1991), Trans. JSME(A), 57-539, 1488.
5. Ochi,Y., Ishii,A., Sasaki,S. and Konishi,Y. (1992), Trans. JSME(A), 58-550, 995.
6. Ochi,Y.,Ogata,T.,Kubota,M and Ishii,A.(1997) Jour. Jap. Soc. Mat. Sci., 46-10, 1155.
7. Hashimoto.M.,Shiratori,M.,Itoh,M. and Hirai,J.(1995), Trans. JSME(A), 61-585, 889.
8. Masaki,K, Ochi,Y. and Ishii,A. (1998), Mat. Sci. Res. Int., 4-3, 200.
9. Yonetani, S. (1975) Generation of Residual Stress and Its Treatment, Yokendo Press.
10. Saruki,K., Yamada,A. and Ogawa,K. (1988) Jour. Jap. Soc. Mat. Sci., 37-417, 631.